A small-molecule therapeutic lead for Huntington's disease: Preclinical pharmacology and efficacy of C2-8 in the R6/2 transgenic mouse

Vanita Chopra*, Jonathan H. Fox*, Greg Lieberman*, Kathryn Dorsey*, Wayne Matson[†‡], Peter Waldmeier[§], David E. Housman[¶‖], Aleksey Kazantsev*, Anne B. Young*, and Steven Hersch*,**

*Department of Neurology, Harvard Medical School, Massachusetts General Hospital, Charlestown, MA 02129; [†]Geriatric Research Education and Clinical Center, Bedford Veterans Affairs Medical Center, Bedford, MA 01730; [‡]Boston University School of Medicine, Boston, MA 02180; [§]Novartis Institute for Biomedical Research, CH-4002 Basel, Switzerland; and [¶]Center for Cancer Research, Massachusetts Institute of Technology, 77 Massachusetts Avenue, Cambridge, MA 02139

Contributed by David E. Housman, August 22, 2007 (sent for review June 1, 2007)

Huntington's disease (HD) is a progressive neurodegenerative disease caused by a glutamine expansion within huntingtin protein. The exact pathological mechanisms determining disease onset and progression remain unclear. However, aggregates of insoluble mutant huntingtin (mhtt), a hallmark of HD, are readily detected within neurons in HD brain. Although aggregated polyglutamines may not be inherently toxic, they constitute a biomarker for mutant huntingtin useful for developing therapeutics. We previously reported that the small molecule, C2-8, inhibits polyglutamine aggregation in cell culture and brain slices and rescues degeneration of photoreceptors in a *Drosophila* model of HD. In this study, we assessed the therapeutic potential of C2-8 in the R6/2 mouse model of HD, which has been used to provide proof-of-concept data in considering whether to advance therapies to human HD. We show that, at nontoxic doses, C2-8 penetrates the blood–brain barrier and is present in brain at a high concentration. C2-8-treated mice showed improved motor performance and reduced neuronal atrophy and had smaller huntingtin aggregates. There have been no prior drug-like, non-toxic, brain-penetrable aggregation inhibitors to arise from cell-based high-throughput screens for reducing huntingtin aggregation that is efficacious in preclinical *in vivo* models. C2-8 provides an essential tool to help elucidate mechanisms of neurodegeneration in HD and a therapeutic lead for further optimization and development.

huntingtin | neuroprotection | protein aggregates

Huntington's disease (HD) is a fatal autosomal dominant neurodegenerative disease caused by a glutamine-coding CAG expansion within exon 1 of the huntingtin gene (1). HD is characterized clinically by progressive motor, psychiatric, cognitive, and functional decline resulting from neurodegeneration particularly in the striatum and cerebral cortex (2–4). As a result of its N-terminal polyglutamine expansion, mutant huntingtin is misfolded and deposited as a component of insoluble protein aggregates that persist in neuronal nuclei, perikarya, and processes (5–7). Although most evidence suggests that huntingtin's toxicity resides in its soluble protein–protein interactions, huntingtin aggregates mark the presence of misfolded mutant huntingtin in vulnerable cell populations and are a hallmark of HD in humans (7) and in genetic *in vivo* (6, 8, 9) and *in vitro* (10) models of HD. Antioxidant and energy buffering compounds, such as coenzyme Q10 (11, 12), creatine (13–15), and cystamine (16, 17), which are neuroprotective in HD transgenic mice, significantly reduce huntingtin aggregates. Aggregation occurs *in vivo* in the presence of expressed polyglutamine-containing proteins, such as huntingtin or huntingtin fragments and adaptation to high-throughput screening has enabled the identification of selective inhibitors (18, 19). The small molecule C2-8 was identified in a high-throughput screen using a yeast-based aggregation assay and was observed to partially inhibit polyglutamine-mediated aggregation in cell culture and brain slices, and rescue photoreceptor degeneration in a *Drosophila* model of HD (20). Furthermore, C2-8 was predicted to have favorable drug-like qualities. In this report, we establish C2-8 as a therapeutic lead compound by investigating its pharmacokinetics, brain bioavailability, and efficacy in the R6/2 transgenic mouse model of HD.

Results

C2-8 Is a Drug-Like Small Molecule That Crosses the Blood–Brain Barrier. C2-8 has poor aqueous solubility. Its high clogP (5.6) and logP (5.2) values are consistent with its low aqueous solubility. It is also relatively insoluble in carboxymethylcellulose and a series of different cyclodextrins (α-cyclodextrin, β-cyclodextrin, hydroxypropyl-β-cyclodextrin, hydroxypropyl-γ-cyclodextrin, octakis-6-iodo-6-deoxy-γ-cyclodextrin, octakis-6-bromo-6-deoxy-γ-cyclodextrin, and octakis-6(dimethyl-tert-butyl-silyl)-γ-cyclodextrin). However, C2-8 can form a fine suspension in 2% chremophore, corn oil, or a universal vehicle provided by Novartis (Basel, Switzerland) that can be administered orally by gavage. For our initial pharmacokinetic (PK) studies, we used wild-type mice. Mice ($n = 5$) were administered 50 mg/kg C2-8 for 5 days. Five hours after the last dose, levels of C2-8 in the brain were determined (Fig. 1*A*). The mean concentration of C2-8 in the cerebral cortex was 25 μM. This is significantly higher than the IC_{50} value of C2-8 in PC12 cells [$IC_{50} = 0.05$ μM (20)]. In parallel studies, mice were administered different doses of C2-8 (5, 10, 25, and 50 mg/kg), and brain and plasma levels were determined at different postdosing intervals (Fig. 1*B*). We found good brain and plasma exposure with a half-life of $\approx$1.5 h for plasma and slightly higher for the brain (1.6–1.9 h). When 10 and 25 mg/kg C2-8 were used, brain and plasma concentrations were below the level of detection at 16 and 24 h (15 and 3 pmol/g respectively). Based on these results, we determined that dosing twice daily would maintain acceptable brain levels over a 24-h period.

We then performed acute and chronic tolerability studies in adult R6/2 mice. Mice ($n = 5$) were dosed daily with a starting

Author contributions: V.C. and J.H.F. contributed equally to this work; V.C., J.H.F., D.E.H., A.B.Y., and S.H. designed research; V.C., J.H.F., G.L., K.D., W.M., and P.W. performed research; V.C. and J.H.F. analyzed data; and V.C., J.H.F., A.K., and S.H. wrote the paper.

The authors declare no conflict of interest.

Abbreviation: HD, Huntington's disease.

‖To whom correspondence may be addressed. E-mail: dhousman@mit.edu.

**To whom correspondence may be addressed at: Department of Neurology, Harvard Medical School, Massachusetts General Hospital, B114 16th Street, Charlestown, MA 02129. E-mail: hersch@helix.mgh.harvard.edu.

This article contains supporting information online at www.pnas.org/cgi/content/full/0707842104/DC1.

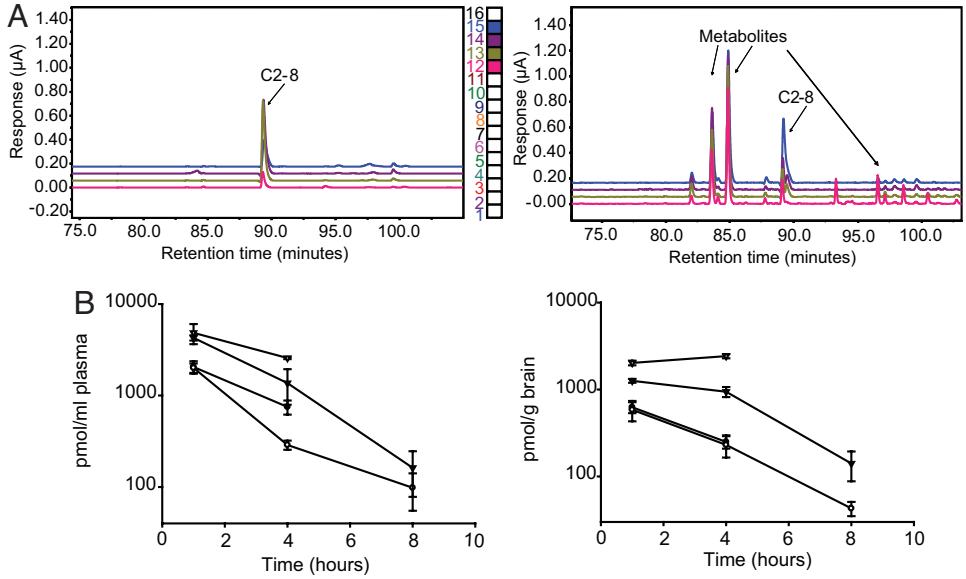

Fig. 1. C2-8 has brain bioavailability at nontoxic doses. (*A*) Gradient chromatography coupled with 16-channel colorimetric array detection enabled the detection of C2-8 in mouse brain. (*Left*) Chromatogram showing C2-8 standard (0.8 μg/ml). The peaks were detected in channels 12–15 at ≈90-min retention time. The analytical values were determined from total integrated values of peaks from channel 12–15. (*Right*) Chromatogram shows brain levels of C2-8 in wild-type mice receiving 50 mg/kg C2-8 p.o. for 5 days. Five hours after the last dose, levels of C2-8 were determined in cortex based on comparison with standards and found to be 25 μM. (*B*) Brain and plasma levels of C2-8 in wild-type mice after single p.o. administration of 5 (filled circle), 10 (open circle), 25 (filled triangle), and 50 (open triangle) mg/kg C2-8. Levels were determined 1, 4, and 8 h after dosing. $n = 5$. Error bars represent SD.

dose of 100 mg/kg that was logarithmically scaled to 800 mg/kg over 11 days. We found no effect on body weight in this study, indicating that C2-8 is not toxic at these doses (data not shown). For chronic tolerability studies, mice ($n = 10$ per treatment group) were administered C2-8 at dose rates of 50, 100, and 200 mg/kg/12 h for 4 weeks. There was no effect on body weight, showing that all these doses were well tolerated (data not shown). Based on the results of our pilot PK and tolerability studies, we designed a dosing regimen for an experiment testing C2-8's efficacy for neuroprotection, in R6/2 mice (below).

We also screened C2-8 against a panel of 60 pharmacologically relevant receptors, ion channels, and transporters expressed in the mammalian brain. The receptor-binding profile revealed IC_{50} values >10 μM, except for dopamine transporter (IC_{50} = 1.7 μM), opioid receptor (IC_{50} = 2.79 μM), and adenosine A3 (IC_{50} = 5.76 μM). The favorable pharmacokinetic profile, including good oral bioavailability, suggests that C2-8 has properties that make it suitable for preclinical and clinical stages of drug development.

C2-8 Reduces the Decline in Motor Performance in R6/2 Mice. We next evaluated the therapeutic potential of C2-8 in R6/2 mice. Mice were administered C2-8 at the dose rate of 100 or 200 mg/kg/12 h. Treatments were started from 24 days of age and continued until spontaneous death or killing. We found that C2-8-treated mice performed better than vehicle controls on the rotarod at 8 and 11 weeks of age (Fig. 2*A*). Latency to fall was increased by 37% at 8 weeks of age (placebo-treated mice = 148 s, C2-8-treated mice = 235 s) and by 43% at 11 weeks of age (placebo-treated mice = 72 s, C2-8-treated mice = 127 s). Consistent with the improvement in the motor performance, we observed significant improvement in wire-hang endurance of C2-8-treated mice at 9.5 and 12.5 weeks of age ($P = 0.0365$ at 9.5 weeks and $P = 0.0002$ at 12.5 weeks, Fig. 2*B*). The wire-hang endurance of C2-8-treated mice (100 mg/kg/12 h) at 12.5 weeks of age (164 s)

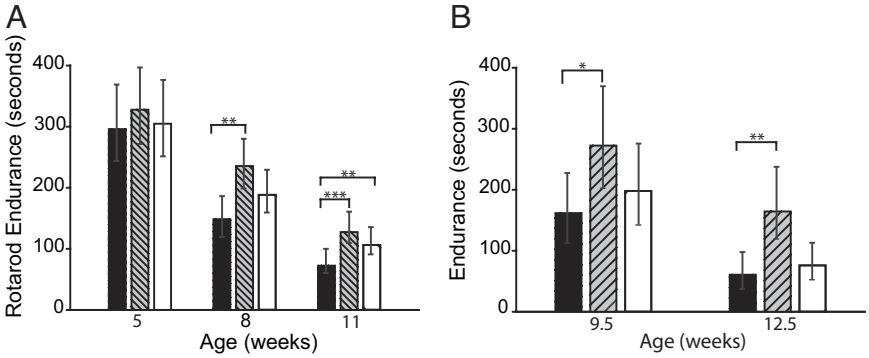

Fig. 2. C2-8 treatment ameliorates behavioral deficits in R6/2 mice. (*A*) Rotarod performance of C2-8-treated and placebo-treated R6/2 mice at 5, 8, and 11 weeks of age. C2-8-treated mice performed better than vehicle controls on the rotarod at 8 and 11 weeks of age. (*B*) Wire-hang endurance of R6/2 mice is significantly improved at 9.5 and 12.5 weeks of age with C2-8 treatment. Black, gray, and white bars represent R6/2 mice treated with 0, 100, or 200 mg/kg/12 h C2-8, respectively. Values represent geometric mean ± 95% confidence interval. $n = 15$; *, $P < 0.05$; **, $P < 0.01$; ***, $P < 0.001$.

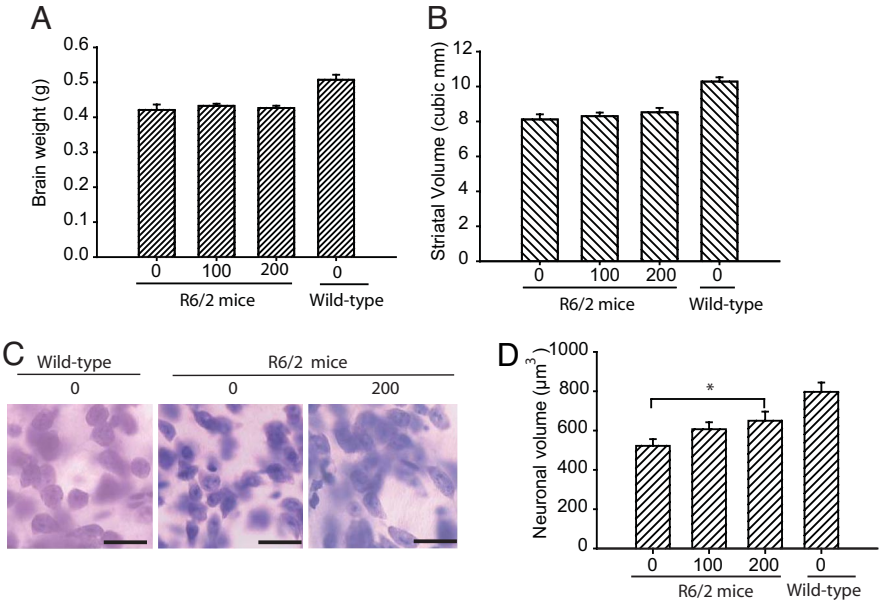

Fig. 3. C2-8 increases striatal neuronal cell body volume in R6/2 mice. (*A* and *B*) C2-8 treatment has no effect on brain weight and striatal volume in R6/2 mice. (*C*) Thionin-stained sections of neostriatum from a wild-type littermate mouse (*Right*), a placebo-treated R6/2 mouse (*Center*), and a C2-8-treated R6/2 mouse (*Left*) at 13 weeks of age. There is evidence of neuronal atrophy in the untreated R6/2 mouse with relative preservation of neuronal atrophy in the C2-8-treated mouse. (Scale bars, 25 μm.) (*D*) Stereological quantification of striatal neuronal cell body volume. Neuronal volume is significantly reduced in R6/2 mice as compared with wild-type littermates. C2-8 treatment partially rescues the loss of striatal neuronal cell body volume in a dose-dependent manner. Error bars represent SEM, $n = 10$; *, $P < 0.05$.

was similar to the performance of placebo-treated mice (161 s) at 9.5 weeks of age, suggesting that motor dysfunction was delayed by 3 weeks by C2-8 treatment. Although C2-8 treatment ameliorated the motor dysfunction in R6/2 mice, it did not affect weight loss or survival [supporting information (SI) Fig. 5 *A* and *B*].

C2-8 Decreases Striatal Neuronal Atrophy in R6/2 Mice. Human HD and R6/2 brain is characterized by atrophy of the neostriatum. We previously demonstrated that C2-8 treatment suppresses photoreceptor degeneration in a *Drosophila* model of HD (20). Here, we examined whether C2-8 treatment decreases gross striatal and neuronal atrophy in R6/2 mice. There was no difference in mean brain weight between C2-8-treated and placebo-treated mice (Fig. 3*A*). However, R6/2 brain weights were significantly lower than those of wild-type mice ($P < 0.001$). Both placebo- and C2-8-treated R6/2 mice had smaller striatal volumes (8.5 $\pm$ 0.2 mm^3 and 8.1 $\pm$ 0.3 mm^3, respectively) as compared with wild-type littermates (10.3 $\pm$ 0.2 mm^3) (both $P <$ 0.05) (Fig. 3*B*). We then estimated striatal neuronal volumes using the nucleator method (see *Materials and Methods*). There was significantly less mean striatal neuronal volume in vehicle-treated R6/2 compared with wild-type mice ($P < 0.001$). Importantly, C2-8 treatment resulted in a significant reduction in neuronal atrophy in the 200 mg/kg C2-8 group ($P < 0.05$) (Fig. 3 *C* and *D*). The average volume of striatal neuronal cell bodies in wild-type mice was 797 $\pm$ 47.5 μm^3, as compared with 522 $\pm$ 34.2 μm^3 in 13-week-old R6/2 mice ($P < 0.0001$). C2-8-treated (200 mg/kg) R6/2 mice had a mean striatal neuronal cell body volume of 650 $\pm$ 46.3 μm^3, which was significantly greater (20%) than placebo-treated R6/2 control mice ($P = 0.0382$).

C2-8 Reduces Striatal Nuclear Aggregate Volume in R6/2 Mice. Microscopically visible huntingtin aggregates are a hallmark of HD and may play an important role in disease progression. In R6/2 mice, intranuclear aggregates are much larger than neuropil aggregates and amenable to quantification using the nucleator method. We examined the effect of C2-8 on polyglutamine aggregates in the striatum of R6/2 mice after immunostaining with EM-48 antibody. In C2-8-treated (200 mg/kg) mice, the intranuclear aggregates appeared somewhat smaller in size than in the placebo-treated R6/2 mice (Fig. 4*A*). These observations were confirmed by stereological quantification of striatal neuronal nuclear aggregate volume by using the nucleator method.

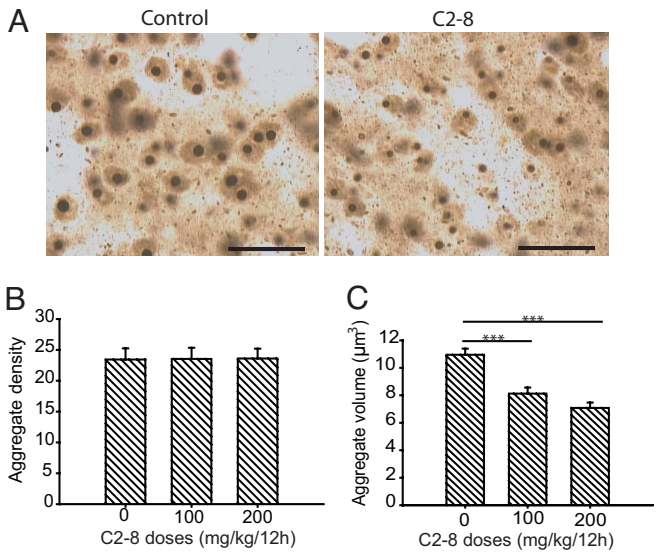

Fig. 4. C2-8 decreases size of neuronal intranuclear huntingtin aggregates. (*A*) Immunodetection of intraneuronal huntingtin aggregates by using EM48 antibody in the neostriatum of 13-week-old R6/2 mice with and without C2-8 treatment. (Scale bars, 25 μm.) (*B*) Stereological counts of striatal intraneuronal aggregates in R6/2 mice. C2-8 treatment had no effect on aggregate density. (*C*) C2-8 treatment significantly reduced the striatal nuclear aggregate volume in R6/2 mice. Error bars indicate SEM, $n = 10$; ***, $P < 0.001$.

There was no effect of C2-8 on nuclear aggregate density (Fig. 4*B*), but we found a significant (35%) reduction in striatal nuclear aggregate volume in C2-8-treated (200 mg/kg) mice as compared with vehicle-treated R6/2 mice (Fig. 4*C*). The mean nuclear aggregate volume in C2-8-treated mice was 7.14 + 0.3 μm^3, as compared with 10.89 + 0.8 μm^3 in placebo-treated R6/2 mice ($P < 0.0001$).

Discussion

Protein aggregation occurs in cells expressing mutant huntingtin, its N-terminal fragments, or other expanded polyglutamine proteins and is readily used for high-throughput screening to discover compounds able to modulate it. Enthusiasm for such assays has been tempered by extensive *in vivo* and *in vitro* data suggesting that huntingtin aggregates are not the most toxic form of mutant huntingtin. Nevertheless, huntingtin aggregation acts as a phenotypic readout that can reflect pathologically relevant processes such as huntingtin cleavage, misfolding, proteolysis, transglutaminase activity, oxidative stress, and protein sequestration. Accordingly, there has been extensive activity seeking potentially therapeutic compounds by using polyglutamine aggregation screening assays. This is the first demonstration that these cell-based screens can produce small, drug-like molecules with brain bioavailability and therapeutic effects *in vivo* in HD transgenic mice.

C2-8 is a small molecule that was identified in a yeast-based screen for inhibitors of polyglutamine aggregation. Early studies demonstrated that it potently inhibits mutant huntingtin aggregation in cell-based models and in brain slice cultures. C2-8 also rescued photoreceptor degeneration in a *Drosophila* model of HD (20). In the present study, we evaluated the potential of C2-8 as a therapeutic lead compound by examining its drug-like properties, including its potential for oral administration, brain bioavailability, off-target pharmacologic interactions, tolerability, and efficacy in the R6/2 mouse model of HD. We found that C2-8 was nontoxic, available orally, had favorable brain pharmacokinetics, had no concerning pharmacologic interactions, reduced huntingtin aggregate size *in vivo*, and was modestly neuroprotective as measured by behavior and neuropathology. Although C2-8 improved motor performance and delayed the motor impairment by ≈3 weeks in R6/2 mice, there was no effect on survival. This suggests that C2-8 may have limited potency or that its activity may be most relevant too early in pathogenesis to be as effective in the R6/2 mouse, in which huntingtin aggregates are already present at birth (21).

Our stereological studies revealed that C2-8 significantly reduced striatal neuronal nuclear aggregate volume, yet the compound had no effect on aggregate number. C2-8 might thus affect aggregate growth but not initiation. These results are in agreement with previous *ex vivo* studies in brain slices, suggesting compound-dependent modulation of aggregation by the same mechanism. This raises the possibility that C2-8 might be more effective when administered before aggregation begins. However, the observed potency of C2-8 for suppressing aggregation in the brain was also much less than in brain slices. This discrepancy may be explained by the rapid metabolism of C2-8 that occurs in mice as revealed in our pharmacokinetics study (Fig. 1*A*).

Given the high C2-8 brain concentration necessary to achieve an inhibitory effect on aggregation, it is conceivable that C2-8 directly blocked formation of inclusions *in vivo*. In a previous study, the IC_{50} of C2-8 *in vitro* was determined as 25 μM, which was in a range of achieved brain concentrations in our *in vivo* studies. The mechanism of aggregation suppression is more likely indirect and depends on modulation of huntingtin levels or of biochemical processes that modulate aggregation. R6/2 mice develop significant striatal cell body atrophy, a manifestation of the gradual neurodegeneration they undergo. Striatal cell volume was 20% greater in C2-8-treated animals; confirming that the phenotypic benefits of C2-8 are likely due to the preservation of neuronal structure and function. This neuroprotective effect was correlated with a 30% reduction in aggregate volume. A number of compounds that have previously been shown to be neuroprotective in R6/2 mice, such as creatine, coenzyme Q10, and cystamine, also suppress huntingtin aggregates. Transcriptionally active compounds that are neuroprotective, such as sodium butyrate (22), sodium phenyl butyrate (23), and mithramycin A (24), do not. However, these compounds may work further downstream, rescuing sick neurons despite the presence of aggregates and the molecular forms of mutant huntingtin that precede them. Consistent with this possibility, unlike C2-8, they have not been selected in aggregate inhibition screens.

The present study validates the use of aggregation suppressors as a phenotypic screen for compounds that have the potential to be neuroprotective in HD. Mechanisms of neuroprotection by C2-8, or possibly by one of its metabolites, remain to be elucidated and could shed light on the relevance of aggregates to HD pathogenesis. C2-8 may not be sufficiently potent in comparison with other neuroprotective agents such as creatine, coenzyme Q10, cystamine, and sodium butyrate to invest in its development as-is for clinical use in HD. However, its benefits and drug-like properties are exciting and support developing more potent or more stable analogs based on the identified structural scaffold. Promising C2-8 derivatives should be explored and assessed in HD transgenic mice to compare their properties. To expedite the discovery of these molecules, identification of the molecular target of C2-8 is also a priority and would permit the rational design of more potent compounds. Target seeking could include testing the binding affinity of radio-labeled C2-8 to a protein panel, biochemical profiling against neuronal enzymes and receptors, and *in silico* comparison with known ligands.

Materials and Methods

Animals. Female R6/2 mice used in the study were generated by back-crossing male R6/2 (available from The Jackson Laboratory, Bar Harbor, ME) with C57BL/6 × CBA F_1 females. Mice were genotyped by PCR using tail-tip DNA (25) and were housed five per cage under standard conditions with ad libitum access to water and food. To ensure homogeneity of experimental cohorts, mice from the same F generation were systemically assigned to experimental groups such that age, weight, and CAG-repeat lengths were balanced. All animal experiments were carried out in accordance with the National Institutes of Health Guide for the Care and Use of Laboratory Animals and were approved by local animal care committee.

Pharmacokinetics. For the single-time-point study, C2-8 levels in the brain were determined by using a long gradient liquid chromatography electrochemical array (LCECA) system which provides resolution of ≈1500 compounds in most biological matrices (26–28). Briefly, this detection method utilizes a combination of retention time and ratio of response across adjacent detectors as a molecular fingerprint to enable identification of a specific peak in HPLC chromatograms. Concentrations for sample peaks were determined based on comparison with standards. Mice were euthanized by cervical dislocation under deep anesthesia, and the brain tissue was immediately removed and stored at −80°C. Cortical tissue (20–30 mg) was extracted by sonification in 1 ml of acetonitrile/0.4% acetic acid at −10°C. The slurry was centrifuged for 15 min at 15,000 × *g* at −4°C, and the supernatant was centrifugally evaporated and reconstituted in 100 μl of mobile phase for injection of 5 μl on the LCECA system. For standard, 0.8 μg/ml C2-8 was used.

For the time-course study, plasma and brain levels of C2-8

were determined by an HPLC/MS method, the details of which are provided in *SI Text*.

Drug Treatment. Compound C2-8 (purity >95%) and the vehicle were obtained from the Novartis Institute for Biomedical Research. Mice were administered different doses of C2-8 orally by gavage twice daily starting from 3 weeks of age. The drug suspension was made fresh daily. Body weights were recorded weekly at the same time of day. Mice were assessed for morbidity and mortality twice daily. The criterion for euthanasia was the point in time when mice could no longer right themselves within 30 seconds after being placed on their sides. Treatment with C2-8 continued until death. Deaths that occurred overnight were recorded the following morning.

Behavioral Analyses. Motor performance was assessed by using an accelerating rotarod (Stoelting, Ugo Basile, Biological Research apparatus; Varese, Italy) at 5, 8, and 11 weeks of age. At the beginning of each week, mice ($n = 15$) were trained for 30 s at a slow speed of 4.5 rpm. Subsequently, three trials were performed for three consecutive days. In each trial, mice were placed onto the rotarod at a constant speed of 4.5 rpm for 5 s, which then accelerated at a constant rate until a terminal angular velocity of 45 rpm was reached. The latency to fall from the rotarod was recorded for each mouse, and the average of three trials was used for statistical analysis. Wire-hang endurance was tested at 9.5 and 12.5 weeks of age. For this, mice were placed on a horizontal wire mesh that was then gently inverted. The time that each mouse remained on the wire was recorded. Three trials were performed for each mouse for three consecutive days, and the average was used for statistical analysis. Data were analyzed by using the mixed procedure in SAS version 8.2 software. Results were considered statistically significant at $P < 0.05$.

Histology. At 90 days of age, mice were deeply anesthetized and then transcardially perfused with 2% paraformaldehyde in 0.1 M phosphate buffer (pH 7.4). Brains were postfixed with perfusant for 2 days, cryoprotected in a graded series of 10% and 20% glycerol/2% DMSO, and serially sectioned at 50 μm by using a SM 2000R freezing microtome (Leica, Wetzlar, Germany). Every eighth section was stained with thionin for striatal volume and neuronal volume analysis. For immunohistochemistry, floating sections of forebrain at the level of crossing of the anterior commissure were stained with EM48 (dilution, 1:2,000) for 2 days, washed, and incubated with biotinylated secondary antibody. Reactivity was developed by using the Vectastain ABC kit (Vector Laboratories, Burlingame, CA). Sections were mounted in aqueous solution (Fluoromount G; Southern Biotech, Birmingham, AL) to prevent z axis shrinkage. No signal was detected in the controls in which primary antibody was omitted. Data were analyzed by ANOVA using the GLM procedure in SAS software. Results were considered statistically significant at $P < 0.05$.

Stereology. All analyses were performed blind by using unbiased stereological approaches, StereoInvestigator software (MicroBrightField, Williston, VT), and a Leica DMLB microscope with a motorized stage. Striatal volumes were estimated on every eighth coronal section by using the Cavalieri method. Stereological counts of aggregate number and volumes of cell bodies and intranuclear aggregates were obtained from the neostriatum at the level of the anterior commissure by using the optical fractionator and nucleator methods, respectively (29). For the optical fractionator, the total area of the right striatum was outlined by using a ×5 objective. The number of aggregates was then counted in a 30 × 30 × 20-μm 3D counting frame using a ×100 objective such that ≈30 frames were counted per striatal section. For cell and aggregate volume estimation, the four-point vertical nucleator was used. The volumes were measured by using the following formula: $V_N = [4\pi/3]l_n^3$, where l is the length of intercept, V_N is the number-weighed volume, and n is the number of nucleator estimates (30). On average, 100 neurons were counted per mouse. Data were analyzed by ANOVA.

We thank Graeme Bilbe and Kaspar Zimmermann for coordinating the contributions from the Novartis Institute for Biomedical Research and assisting with the manuscript. This study was supported by the Discovery of Novel Huntington's Disease Therapeutics Fund (A.B.Y.), MassGeneral Institute for Neurodegenerative Disease, Massachusetts General Hospital.

1. The Huntington's Disease Collaborative Research Group. (1993) *Cell* 72:971–83.
2. Gusella JF, MacDonald ME (2000) *Nat Rev Neurosci* 1:109–15.
3. Bates G, Harper P, Jones L (2002) *Huntington's Disease* (Oxford Univ Press, New York).
4. Hersch SM, Rosas HR, Ferrante RJ (2004) in *Movement Disorders: Neuropathologic Principles and Practice*, eds Watta RL, Koller WC (McGraw–Hill, New York), pp 503–523.
5. Mangiarini L, Sathasivam K, Seller M, Cozens B, Harper A, Hetherington C, Lawton M, Trottier Y, Lehrach H, Davies SW, Bates GP (1996) *Cell* 87:493–506.
6. Davies SW, Turmaine M, Cozens BA, DiFiglia M, Sharp AH, Ross CA, Scherzinger E, Wanker EE, Mangiarini L, Bates GP (1997) *Cell* 90:537–48.
7. DiFiglia M, Sapp E, Chase KO, Davies SW, Bates GP, Vonsattel JP, Aronin N (1997) *Science* 277:1990–3.
8. Lunkes A, Mandel JL (1998) *Hum Mol Genet* 7:1355–61.
9. Warrick JM, Paulson HL, Gray-Board GL, Bui QT, Fischbeck KH, Pittman RN, Bonini NM (1998) *Cell* 93:939–49.
10. Scherzinger E, Lurz R, Turmaine M, Mangiarini L, Hollenbach B, Hasenbank R, Bates GP, Davies SW, Lehrach H, Wanker EE (1997) *Cell* 90:549–58.
11. Ferrante RJ, Andreassen OA, Dedeoglu A, Ferrante KL, Jenkins BG, Hersch SM, Beal MF (2002) *J Neurosci* 22:1592–9.
12. Smith KM, Matson S, Matson WR, Cormier K, Del Signore SJ, Hagerty SW, Stack EC, Ryu H, Ferrante RJ (2006) *Biochim Biophys Acta* 1762:616–26.
13. Ferrante RJ, Andreassen OA, Jenkins BG, Dedeoglu A, Kuemmerle S, Kubilus JK, Kaddurah-Daouk R, Hersch SM, Beal MF (2000) *J Neurosci* 20:4389–97.
14. Andreassen OA, Dedeoglu A, Ferrante RJ, Jenkins BG, Ferrante KL, Thomas M, Friedlich A, Browne SE, Schilling G, Borchelt DR, *et al.* (2001) *Neurobiol Dis* 8:479–91.
15. Dedeoglu A, Kubilus JK, Yang L, Ferrante KL, Hersch SM, Beal MF, Ferrante RJ (2003) *J Neurochem* 85:1359–67.
16. Dedeoglu A, Kubilus JK, Jeitner TM, Matson SA, Bogdanov M, Kowall NW, Matson WR, Cooper AJ, Ratan RR, Beal MF, *et al.* (2002) *J Neurosci* 22:8942–50.
17. Karpuj MV, Becher MW, Springer JE, Chabas D, Youssef S, Pedotti R, Mitchell D, Steinman L (2002) *Nat Med* 8:143–9.
18. Heiser V, Scherzinger E, Boeddrich A, Nordhoff E, Lurz R, Schugardt N, Lehrach H, Wanker EE (2000) *Proc Natl Acad Sci USA* 97:6739–44.
19. Tanaka M, Machida Y, Niu S, Ikeda T, Jana NR, Doi H, Kurosawa M, Nekooki M, Nukina N (2004) *Nat Med* 10:148–54.
20. Zhang X, Smith DL, Meriin AB, Engemann S, Russel DE, Roark M, Washington SL, Maxwell MM, Marsh JL, Thompson LM, *et al.* (2005) *Proc Natl Acad Sci USA* 102:892–7.
21. Stack EC, Kubilus JK, Smith K, Cormier K, Del Signore SJ, Guelin E, Ryu H, Hersch SM, Ferrante RJ (2005) *J Comp Neurol* 490:354–70.
22. Ferrante RJ, Kubilus JK, Lee J, Ryu H, Beesen A, Zucker B, Smith K, Kowall NW, Ratan RR, Luthi-Carter R, Hersch SM (2003) *J Neurosci* 23:9418–27.
23. Gardian G, Browne SE, Choi DK, Klivenyi P, Gregorio J, Kubilus JK, Ryu H, Langley B, Ratan RR, Ferrante RJ, Beal MF (2005) *J Biol Chem* 280:556–63.
24. Ferrante RJ, Ryu H, Kubilus JK, D'Mello S, Sugars KL, Lee J, Lu P, Smith K, Browne S, Beal MF, *et al.* (2004) *J Neurosci* 24:10335–42.
25. Mangiarini L, Sathasivam K, Mahal A, Mott R, Seller M, Bates GP (1997) *Nat Genet* 15:197–200.
26. Matson WR, Langlais P, Volicer L, Gamache PH, Bird E, Mark KA (1984) *Clin Chem* 30:1477–88.
27. Kristal BS, Vigneau-Callahan KE, Matson WR (1998) *Anal Biochem* 263:18–25.
28. Kristal BS, Vigneau-Callahan K, Matson WR (2002) *Methods Mol Biol* 186:185–94.
29. Moller A, Strange P, Gundersen HJ (1990) *J Microsc* 159:61–71.
30. Gundersen (1988) *J Microsc* 151:3–21.